Available online at www.sciencedirect.com

SCIENCE DIRECT

Surface & Coatings Technology 200 (2005) 448–452

SURFACE & COATINGS TECHNOLOGY

www.elsevier.com/locate/surfcoat

Increasing the deposition rate of oxide films by increasing the plasma reactivity

R. Snyders*, R. Gouttebaron, J.P. Dauchot, M. Hecq

Laboratoire de Chimie Inorganique et Analytique, Université de Mons-Hainaut, Bâtiment Materia Nova, Park Initialis, Avenue Copernic, 7000 Mons, Belgium

Available online 31 March 2005

Abstract

One of the major problems of reactive sputtering is the dramatically deposition rate decrease when the target surface is poisoned. For decades, numerous papers have been published in order to solve this problem using the same basic idea: prepare a compound film while the target remains non-poisoned. In this work, we propose an original way to reach this goal. From previous results, we have shown that the substrate oxidation occurs mainly by the reactive gas atomic species. In order to favour this reaction we have increased the plasma reactivity by a RF coil located between the DC magnetron target and the substrate. We have studied three reactive systems: Sn–Ar/O_2, Ti–Ar/O_2 and Ag–Ar/O_2. For each of these systems, we have estimated the RF coil influence on the chemical behavior of both the discharge and the films. The discharge is characterized by mass spectrometry measurements whereas the films' compositions are obtained by XPS. Increasing the RF coil power, we observe an increase of the oxygen concentration in the films for the same introduced pO_2. On the other hand, the target metal-compound transition, observed on the deposition rate measurements, is not influenced by the amplification. So, using the RF coil, the fully oxidized films is reached at lower reactive gas flow and consequently at higher deposition rate.

Keywords: Reactive sputtering; RF coil amplification; Deposition rate

1. Introduction

Reactive sputtering is commonly used for thin compound films deposition. It is commonly accepted that reactive deposition occurs by a double mechanism, which consists of the sputtered compound condensation and the reaction between the deposited compound and the plasma reactive species [1,2]. Previously, we have studied the tin [3], silver [4] and titanium [5] oxide reactive sputtering in pure magnetron discharges. We have shown the relative importance of these two mechanisms. Depending on the metal, 80% (titanium), 35% (tin) and 5% (silver) of the oxygen present in the films come from the target sputtering/condensation mechanism. The remainder needed to reach the final stoichiometry reacts on the substrate with the deposited compound. On the other hand, we have shown that the main specie, which oxidizes the substrate, is the atomic oxygen. In this paper, we have taken an interest on the metal oxide thin films synthesis in RF coil amplified discharges. The discharge amplification consists mainly of higher plasma ionisation and dissociation level [6–9]. The film composition is measured by X-ray photoemission spectroscopy (XPS), the plasma composition by both glow discharge mass spectrometry (GDMS) and neutral mass spectrometry (RGA) and the deposition rate by a quartz microbalance.

2. Experimental setup

Metal oxide films are deposited on silicon wafers by DC magnetron reactive sputtering in a planar magnetron sputtering system which is described elsewhere [10]. Metal (tin, titanium, and silver) disks (99.99% purity) of 2 in. in diameter are used as targets. In order to generate high-density plasma, a simple turn copper coil of diameter 4 cm and thickness 0.6 cm is located at 4 cm above the cathode. The coil is powered by a 13.56 MHz generator (Hüttinger

* Corresponding author.
E-mail address: rony.snyders@polymtl.ca (R. Snyders).

0257-8972/$ - see front matter © 2005 Elsevier B.V. All rights reserved.
doi:10.1016/j.surfcoat.2005.02.067

PFG 300 RF) coupled with a matching netbox (Hüttinger Tunning network PFM 400 A). The deposition rate is measured using a quartz microbalance. Ionic and neutral species coming from the discharge are measured using a Balzers PPM 421 differentially pumped quadrupole mass spectrometer with an integrated energy analyzer [11]. The films' stoichiometry is measured by X-ray photoelectron spectroscopy (XPS). All experiments have been performed under UHV; there is no air contamination before XPS analysis. XPS was performed on a VG-ESCALAB 220iXL spectrometer. The pressure in the analysis chamber was typically $8*10^{-11}$ Torr ($1.066*10^{-8}$ Pa). The XPS data were collected using monochromatised Al Kα radiation at 1486.6 eV. Photoelectrons were collected from a 250*1000 μm^2 sample area at a take-off angle, $\Theta = 0^\circ$ (normal detection) from surface normal. In all samples, survey spectra were recorded with a 50 eV pass energy 150 W electron beam power, as well as the high resolution spectra in the regions of O 1s, Sn 3d, Ti 2p and Ag 3d with a 20 eV pass energy. Atomic composition were derived from peak areas by using photoionisation cross-section calculated by Scofield [12], corrected for the dependence of the escape depth on the kinetic energy of the electrons (assumed to have the form $\lambda = KE^{0.6}$) and corrected for the analyzer transmission function of our spectrometer.

3. Experimental results

Varying the gaseous composition and the RF coil power, we have measured the deposition rate, the discharge composition and the film stoichiometry for each studied systems. The introduced partial pressure in O_2 (pO_2(in)) is calculated from: $pO_2 = \%O_2 * p_{tot}$ and $\%O_2 = \frac{f_{O_2}}{f_{O_2}+f_{Ar}}$. Where p_{tot} is the working pressure and f_{O_2} and f_{Ar}, respectively, are the flows in O_2 and Ar. The experimental conditions are summarized in Table 1.

3.1. Deposition rate evolution vs pO_2(in) for different RF coil power

Fig. 1(a,b,c) show the deposition rate (R_D) evolution vs pO_2(in) for the different systems. In every case, at low pO_2(in), the target is mainly metallic and R_D is high. When pO_2(in) is high enough to form a target compound, R_D decreases dramatically: the target becomes "poisoned" [2–5]. When the RF coil power varies, we observe on Fig. 1(a,b,c) a light R_D decrease due to the target voltage decreasing [10]. On the other hand, the transition between the metallic and the compound mode occurs for the same pO_2(in) for every RF power. We can conclude that the discharge amplification does not influence the target poisoning mechanism.

Table 1
Experimental conditions

Metals	DC current density (mA/cm^2)	RF power (W)	Pressure (mTorr)	Flow (sccm)	Percent (%) O_2
Sn	10	0–200	5	20	0–100
Ti	35	0–200	8	80	0–25
Ag	9.5	0–200	5	20	0–100

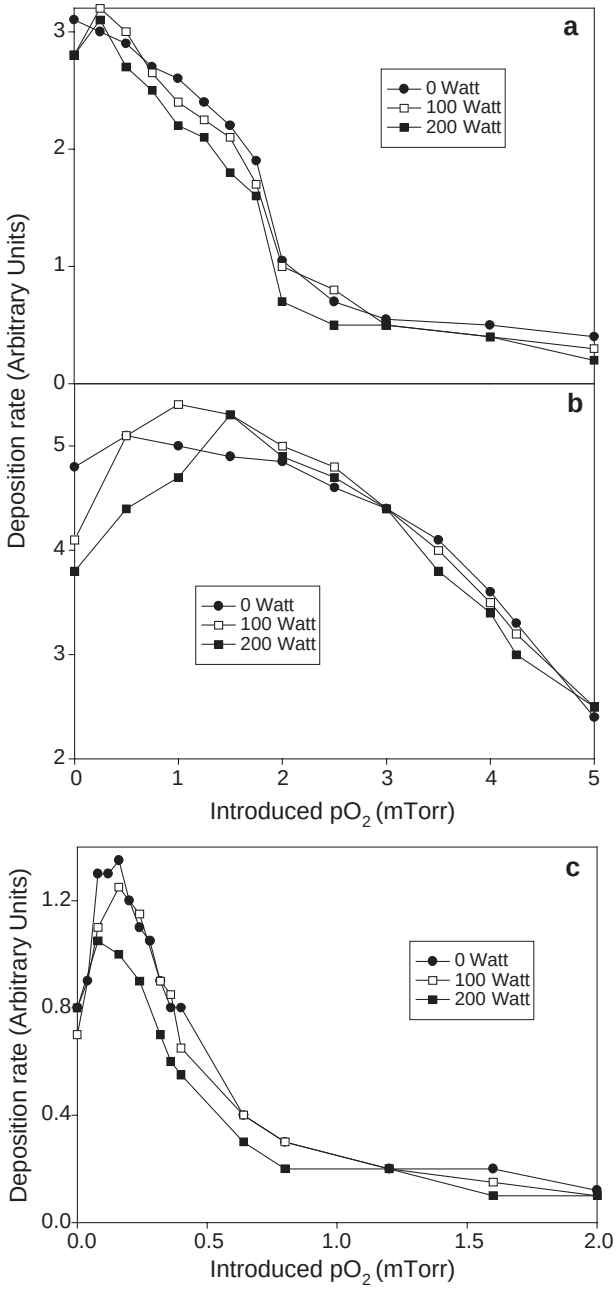

Fig. 1. R_D vs pO_2(in) for different RF powers at the coil (0, 100 and 200 W). (a) Sn–Ar/O_2, (b) Ag–Ar/O_2, and (c) Ti–Ar/O_2.

3.2. Discharge composition by mass spectrometry

3.2.1. O_2 dissociation level by RGA

Due to the very high sticking coefficient of the atomic oxygen [1,13], it is very difficult to estimate its density by RGA. Consequently, we have estimated the O_2 dissociation

level from the O_2 consumption curves. As an example, Fig. 2 shows, for the system Sn–Ar/O_2, the O_2 consumption evolution vs pO_2(in) for different RF coil powers. The O_2 consumption is calculated from:

$$\%O_2\ \text{cons} = \frac{pO_2(\text{in}) - pO_2(\text{eff})}{pO_2(\text{in})}$$

where pO_2(eff) is the effective pO_2. The curve evolutions are similar for every RF coil power. At low pO_2(in), the O_2 consumption is high due to the sputtered metal getter effect. Then, the consumption decreases to reach a plateau when the reactive sputtering dynamic equilibrium is reached. This plateau appears for higher consumed percentage of O_2 when the RF power increases (15% at 0 W, 65% at 100 W, and 78% at 200 W). In magnetron discharge, the O_2 consumption occurs by ionisation, chemical reactions and dissociation [1,14]. For a pure magnetron discharge, the reactive gas ionisation level is around 0.1% [9] and we have estimated the dissociation level at 11% from the model of Bretagne et al. [14]. By difference, the O_2 consumption by chemical reaction is around 4%. When the discharge is amplified, the O_2 ionisation and dissociation levels increase. The O_2 consumption by chemical reaction is close to the level calculated for a pure magnetron discharge [10]. Concerning the O_2 ionisation level, it must be lower than 20% which is the level measured for the metallic species [9] due to the higher ionisation threshold for O_2 (12.15 eV) than for the metallic species (around 7 eV). Considering an O_2 consumption by chemical reaction of 4% and a maximum ionisation level of 20% we can estimate, when the reactive sputtering dynamical equilibrium is reached, a dissociation level of 41% and 54%, respectively, for 100 and 200 W applied at the coil.

3.2.2. Metallic vapour composition by GDMS

Fig. 3 represents the plasma stoichiometry (X_{Plasma}) evolution for the different studied systems. X_{Plasma} is calculated from the molar fractions (x_M) of each metallic species obtained by GDMS [3–5,15] and is defined as the oxygen/metal ratio in the sputtered vapour. X_{Plasma} is given by:

$$X_{\text{plasma}}(\text{Sn}) = \frac{\text{O}}{\text{Sn}} = \frac{x_{\text{SnO}} + 2{*}x_{\text{SnO}_2}}{x_{\text{Sn}} + x_{\text{SnO}} + x_{\text{SnO}_2}}$$

$$X_{\text{plasma}}(\text{Ti}) = \frac{\text{O}}{\text{Ti}} = \frac{x_{\text{TiO}} + 2{*}x_{\text{TiO}_2}}{x_{\text{Ti}} + x_{\text{TiO}} + x_{\text{TiO}_2}}$$

$$X_{\text{plasma}}(\text{Ag}) = \frac{\text{O}}{\text{Ag}} = \frac{x_{\text{AgO}} + x_{\text{Ag}_2\text{O}}}{x_{\text{Ag}} + x_{\text{AgO}} + 2{*}x_{\text{Ag}_2\text{O}}}.$$

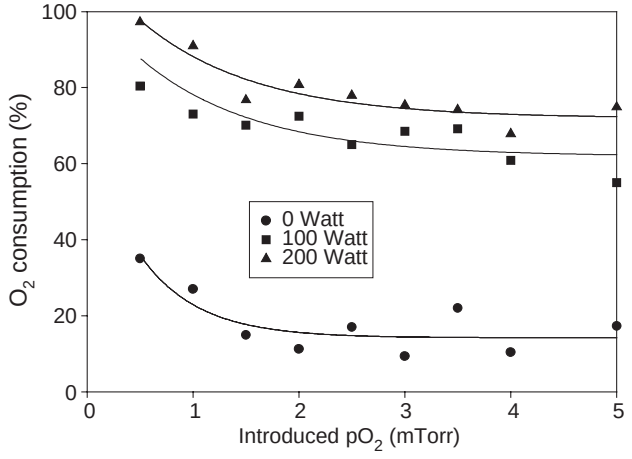

Fig. 2. O_2 consumption by the process vs pO_2(in) for different RF powers at the coil (0, 100 and 200 W), Sn–Ar/O_2 system.

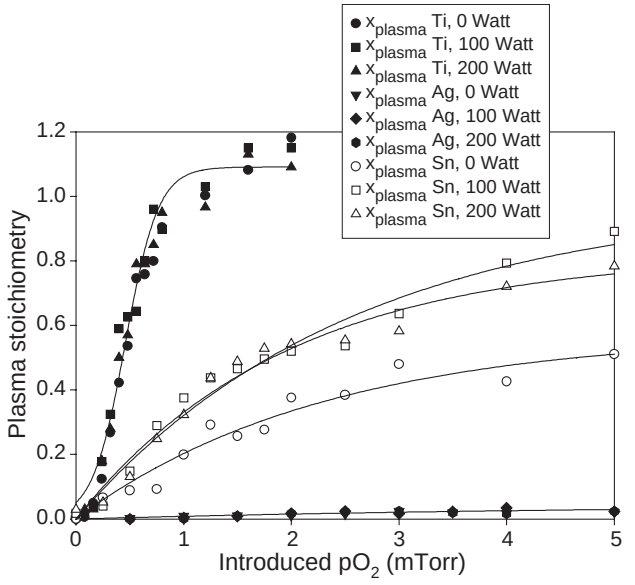

Fig. 3. X_{Plasma} vs pO_2(in) for different RF powers at the coil and for the different systems.

Obviously, for all the studied systems, X_{Plasma} increases with pO_2(in) until a plateau when the reactive sputtering dynamical equilibrium is reached. In the cases of Ti and Ag discharges, we do not observe any amplification influence on X_{Plasma}. This is in agreement with the deposition rate measurements (no RF influence on the poisoning mechanism). On the other hand, curiously, for the tin system, we observe a X_{Plasma} modification due to the RF power. We have interpreted this phenomena considering a process which occurs as an atomic ejection from the target (also absorbed species) and molecular recombination close to the target surface [16,17]. In the case of tin, by discharge voltage measurements, we have measured a reactive species chemisorption increase at the target surface due to the discharge amplification [10]. This chemisorption increase modifies the atomic ejection/molecular recombination process and leads to a modification of X_{Plasma}.

4. Deposited films' stoichiometry

The oxygen concentration in the deposited films is measured by XPS. Fig. 4(a,b,c) show the evolution of

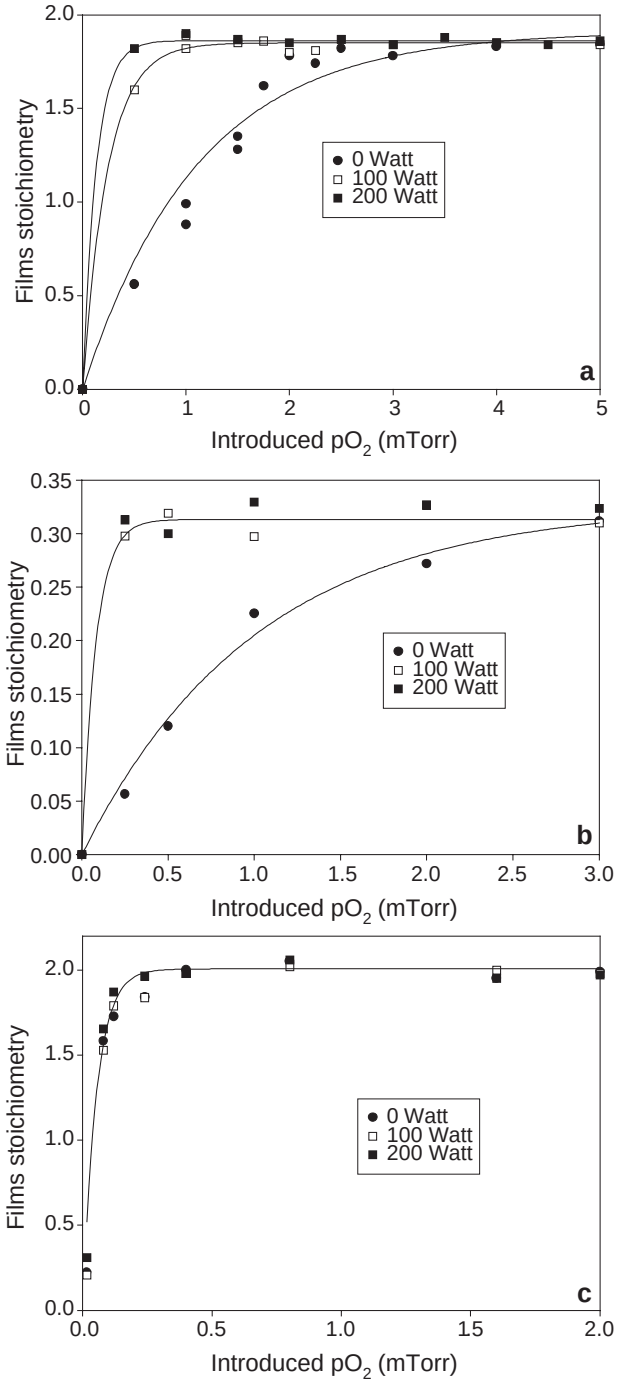

Fig. 4. X_{Film} vs pO_2(in) for different RF powers at the coil (0, 100 and 200 W). (a) Sn–Ar/O_2, (b) Ag–Ar/ O_2, and (c) Ti–Ar/O_2.

the film stoichiometry (X_{Films}) which is defined to be the oxygen/metal atomic ratio in the deposited films. X_{Films} depends mainly on pO_2(in) and, for Ag–Ar/O_2 and Sn–Ar/O_2, on the RF coil power. For every metal and for all the RF powers, X_{Film} increases with pO_2(in) until the final stoichiometry is reached. For Sn–Ar/O_2 and Ag–Ar/O_2, the maximum stoichiometry is reached at lower pO_2(in) when the RF power increases. In these cases, the film oxidation is improved by the amplification. For Ti–Ar/O_2, we do not observe oxidation enhancement due to the RF power. In other words, this system is non-sensitive to the atomic oxygen density increase. We have attributed this observation to the very high reactivity of Ti for O_2 even in a pure magnetron discharge.

5. Discussion

The goal of this work was to produce metal oxide films at high deposition rate. We have shown that, by introducing RF coil plasma between the substrate and the target, we improve the substrate oxidation especially for tin and silver. Fig. 5(a,b) show the comparison between R_D and X_{Film} for Sn–Ar/O_2 discharges, respectively, in a pure magnetron discharge and in a 200 W amplified discharge. The fully oxidized film deposition rate is increased by a factor 6 in the 200 W amplified discharge. Indeed, in the pure magnetron discharge, the full stoichiometry is reached for pO_2(in)=3 mTorr (R_D=0.3) while in the amplified discharge, the full stoichiometry is reached for pO_2(in)= 0.5 mTorr (R_D=1.6). By increasing the plasma reactivity, we favour the reaction between the deposited films and the atomic oxygen by increasing the atomic oxygen density. In the case of silver, we measure a deposition rate increase of

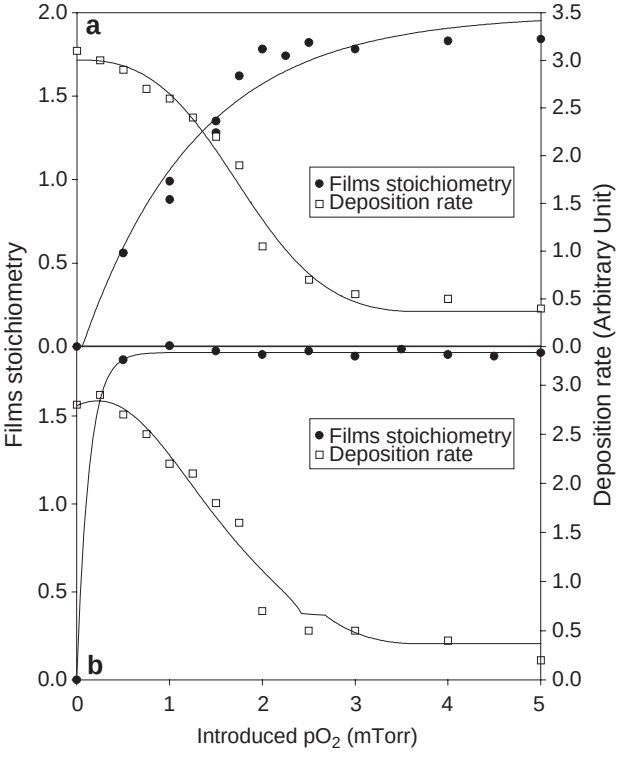

Fig. 5. Tin oxide films' stoichiometry and deposition rate vs pO_2(in). (a) Pure magnetron discharge and (b) 200 W amplified discharge.

50% while in the case of titanium, no modification has been measured.

6. Conclusions

In this work we have investigated the thin metal oxide films deposition by reactive magnetron sputtering in RF coil amplified discharges. We have measured the RF coil influence on the discharge parameters (R_D), on the discharge composition (X_{Plasma}, pO_2(eff)) and on the thin films' stoichiometry. From R_D results, we have shown that the target poisoning is not dependent on the amplification. The GDMS measurements show that, for titanium and silver, the plasma composition is also independent on the RF power. For tin, due to a higher active species chemisorption on the target surface, we observe an increase of X_{Plasma} with the RF power. Nevertheless this chemisorption modification does not modify the target poisoning. Concerning X_{Film}, the XPS measurements show an oxidation improvement with the amplification, especially for tin and silver. We explain these observations by the higher molecular oxygen dissociation due to the amplification (11% at 0 W, 41% at 100 W and 54% at 200 W). In consequence, we favour the compound formation by oxidation on the substrate. Comparing the results, we can conclude that, in this experimental setup, it is possible to produce metal oxide films while the target remains non-poisoned.

References

[1] L. Pekker, Thin Solid Films 312 (1998) 341.
[2] S. Berg, T. Nyberg, H.-O. Blom, C. Nender, Handbook of thin film process technology, IOP, Bristol, 1999.
[3] R. Snyders, M. Wautelet, R. Gouttebaron, J.P. Dauchot, M. Hecq, Thin Solid Films 423 (2003) 125.
[4] R. Snyders, M. Wautelet, R. Gouttebaron, J.P. Dauchot, M. Hecq, Surf. Coat. Technol. 174–175 (2003) 1282.
[5] R. Snyders, M. Wautelet, R. Gouttebaron, J.P. Dauchot, M. Hecq, Proceedings of the 45th Annual Technical Conference of the SVC, 323, Lake Buena Vista, Fl, 2002 (April).
[6] M. Yamashita, Y. Setsuhara, S. Miyake, M. Kumagai, T. Shoji, J. Musil, Jpn. J. Appl. Phys., Part 1 38 (1999) 4291.
[7] K. Nakamura, Y. Kuwashita, H. Sugai, Jpn. J. Appl. Phys., Part 2 34 (1995) L1686.
[8] S.M. Rossnagel, Thin Solid Films 263 (1995) 1.
[9] S. Konstantinidis, C. Nouvellon, J.P. Dauchot, M. Wautelet, M. Hecq, Surf. Coat. Technol. 174–175 (2003) 100.
[10] R. Snyders, R. Gouttebaron, J.P. Dauchot, M. Hecq, J. Vac. Sci. Technol., A, Vac. Surf. Films 22 (2004) 1540.
[11] PPM 421 Handbook, Liechtenstein, Balzers, 1998.
[12] J.H. Scofield, J. Electron. Spectrosc. Relat. Phenom. 8 (1976) 123.
[13] S. Berg, H.-O. Blom, T. Larsson, C. Nender, J. Vac. Sci. Technol., A, Vac. Surf. Films 5 (1987) 202.
[14] W. Trennepohl Jr., J. Bretagne, G. Gousset, D. Pagnon, M. Touzeau, Plasma Sci. Technol. 5 (1996) 607.
[15] R. Snyders, R. Gouttebaron, J.P. Dauchot, M. Hecq, J. Anal. At. Spectrom. 18 (2003) 618.
[16] M. Hecq, A. Hecq, Thins Solid Films 76 (1981) 35.
[17] F. Honda, G.M. Lancaster, Y. Fukuda, J.W. Rabalais, J. Chem. Phys. 69 (1978) 4931.